VER
Vascular & Endovascular Review

Formulation and Evaluation of Transdermal Polyherbal Patch for the Management of Rheumatoid Arthritis

Dr. Gurpreet Singh Sandhu[1], Dr Rohit Mittal[2], Dr. Shiv Jeet Singh[3], Ayushi Srivastava[4], Dr. Paridhi Puri[5], Smita Vasant Nhawkar[6], Dr.Mansi L.Patil[7], Radha Pal[8], Bhagyashree Agrawal[9]

[1]Assistant Professor, Khalsa College of Pharmacy, Amritsar
[2]HOD, University College of Pharmacy, Guru Kashi University, Talwandi Sabo"
[3]Lecturer, Department of Pharmacy, Government Girls Polytechnic, Prayagraj, Uttar Pradesh.
[4]Assistant Professor, Yashraj college of professional studies, Kanpur
[5]Assistant Professor, University Centre for Research and Development, Chandigarh University, Mohali, Punjab, 140413, India.
"
[6] Ashokrao Mane College of Pharmacy, Pethvadgaon Kolhapur
[7]Assistant Professor, TSSM's Jayawant Institute of Pharmaceutical Sciences and Research Bavdhan Pune 411021.
[8]Lecturer, Department of Pharmacy, Government Girls Polytechnic, Prayagraj, Uttar Pradesh.
[9]Assistant Professor JKIPER, Bilaspur Chhattisgarh

Corresponding Author
Bhagyashree Agrawal, Assistant Professor JKIPER, Bilaspur Chhattisgarh bhagyashreeagrawal@rocketmail.com

ABSTRACT

Objective: To design, develop, and evaluate a transdermal polyherbal patch incorporating standardized extracts of Boswellia serrata, Curcuma longa, Zingiber officinale, and Piper nigrum for sustained anti-inflammatory action relevant to rheumatoid arthritis (RA). Methods: Solvent-casting films composed of HPMC/PVP/EC with PEG-400 and permeation enhancers (oleic acid, DMSO, limonene) were optimized by physicomechanical and biopharmaceutical criteria. Comprehensive quality attributes—thickness, weight uniformity, folding endurance, moisture handling, swelling index, tensile strength, drug content, and WVTR—were quantified. In-vitro release, ex-vivo porcine skin permeation (lag time, flux, permeability coefficient), and a protein-denaturation inhibition assay were conducted. Accelerated stability (40°C/75%RH, 3 months) was assessed for the lead batch. Results: Batches F2–F4 met predefined quality targets; F3 exhibited balanced mechanics (tensile strength 33±2 MPa; elongation 32±4%) and sustained release (>75% at 12 h; ~95% at 24 h) with the highest steady-state flux (28.9 µg/cm²/h). Anti-inflammatory potential of polyherbal films approached a standard diclofenac gel in the in-vitro model. Stability of F3 indicated minimal loss of drug content (−1.1% over 3 months) and preserved release. Conclusion: The polyherbal transdermal patch demonstrates robust manufacturability, sustained release, efficient skin transport, and promising anti-inflammatory activity, supporting its potential as an adjunct modality for RA symptom management.

KEYWORDS: Transdermal patch; Polyherbal; Rheumatoid arthritis; Boswellia; Curcumin; Permeation enhancers; HPMC; PVP; Ex vivo permeation.

How to Cite: Gurpreet Singh Sandhu, Rohit Mittal, Shiv Jeet Singh, Ayushi Srivastava, Paridhi Puri, Smita Vasant Nhawkar, Mansi L.Patil, Radha Pal, Bhagyashree Agrawal., (2025) Formulation and Evaluation of Transdermal Polyherbal Patch for the Management of Rheumatoid Arthritis, Vascular and Endovascular Review, Vol.8, No.15s, 354-363

INTRODUCTION

Rheumatoid arthritis (RA) is a chronic, progressive autoimmune disorder characterized by persistent synovial inflammation, cartilage degradation, and bone erosion, ultimately leading to joint deformity and disability. Affecting nearly 1% of the global population, RA imposes substantial socioeconomic and quality-of-life burdens, especially in aging populations and among women in the 40–60-year age group [1,2]. The disease pathogenesis involves complex interplay between genetic susceptibility (HLA-DRB1 alleles, PTPN22 polymorphisms), environmental triggers (smoking, microbiota dysbiosis), and immune dysregulation. Activated antigen-presenting cells stimulate $CD4^+$ T-cells and B-cells, which release cytokines such as tumor necrosis factor-α (TNF-α), interleukin-1β (IL-1β), and interleukin-6 (IL-6). These proinflammatory mediators perpetuate synovial hyperplasia, pannus formation, and matrix metalloproteinase activation, thereby driving cartilage and bone destruction [3,4].

The contemporary therapeutic landscape for RA includes nonsteroidal anti-inflammatory drugs (NSAIDs), corticosteroids, disease-modifying antirheumatic drugs (DMARDs), and biologic response modifiers [5]. While NSAIDs and corticosteroids alleviate pain and inflammation, they do not alter disease progression and carry significant risks such as gastrointestinal bleeding, cardiovascular events, and hepatic toxicity [6]. Conventional DMARDs like methotrexate, leflunomide, and sulfasalazine remain the first line of treatment, but long-term use leads to hepatotoxicity, bone marrow suppression, and intolerance in a considerable subset of patients [7]. Biologics and Janus kinase (JAK) inhibitors have transformed management paradigms but are costly, require parenteral administration, and increase infection risk due to immunosuppression [8,9]. Hence, there remains a persistent

unmet need for alternative or adjunct therapeutic modalities that can mitigate chronic inflammation while minimizing systemic toxicity and improving patient adherence.

Limitations of Oral and Parenteral Therapies

Oral administration of anti-arthritic drugs often suffers from poor and variable bioavailability owing to first-pass metabolism, enzymatic degradation, and gastrointestinal irritation [10]. Frequent dosing further compromises adherence in chronic therapy. Parenteral administration, while bypassing hepatic metabolism, is invasive and associated with injection-site pain, local infections, and low patient acceptability. These pharmacokinetic and compliance challenges have accelerated research into controlled and targeted delivery systems capable of maintaining steady-state plasma levels of therapeutically active compounds with minimal systemic side effects [11].

Rationale for Transdermal Drug Delivery

Transdermal drug delivery systems (TDDS) have emerged as a promising platform to overcome the drawbacks of conventional routes. They offer controlled, non-invasive, and sustained delivery of drugs directly into systemic circulation, bypassing first-pass metabolism and maintaining constant plasma concentrations [12]. The skin, though a formidable barrier, provides a vast surface area for absorption. Formulation design must therefore address the challenge of stratum corneum penetration — the outermost lipid-rich layer that limits the transport of hydrophilic or high-molecular-weight compounds [13]. Advances in polymer science, nanotechnology, and permeation enhancers have revolutionized TDDS, enabling effective delivery of both synthetic and phytopharmaceutical actives [14].

Pharmaceutical polymers such as hydroxypropyl methylcellulose (HPMC) and polyvinylpyrrolidone (PVP) are extensively used to form flexible, transparent, and biocompatible films with good mechanical strength and moisture regulation [15]. Hydrophilic–hydrophobic blends with ethyl cellulose (EC) enable fine-tuning of release kinetics, while plasticizers like polyethylene glycol (PEG-400) enhance flexibility and prevent brittleness. Permeation enhancers such as dimethyl sulfoxide (DMSO), oleic acid, and terpenes temporarily disrupt the ordered lipid structure of the stratum corneum, increasing drug diffusivity and skin flux [16]. These formulation variables can be optimized to achieve sustained, therapeutically relevant release with desirable physicochemical stability.

Transdermal delivery of herbal and polyherbal actives is particularly advantageous because phytoconstituents often suffer from poor oral bioavailability due to low aqueous solubility, instability in gastric pH, and extensive hepatic metabolism [17]. Delivering these bioactives through the skin avoids gastrointestinal degradation, enhances bioefficacy, and provides a steady plasma concentration profile conducive to chronic disease management.

Rationale for Polyherbal Approach in RA

Phytomedicine plays an integral role in modern drug discovery and integrative healthcare. Several botanicals possess anti-inflammatory, antioxidant, and immunomodulatory properties relevant to RA pathophysiology [18]. The current research integrates standardized extracts of *Boswellia serrata*, *Curcuma longa*, *Zingiber officinale*, and *Piper nigrum* in a synergistic transdermal platform. The rationale for this combination lies in their complementary molecular mechanisms and pharmacodynamic interactions that target multiple inflammatory pathways simultaneously.

Boswellia serrata (Salai guggul) resin contains boswellic acids—particularly 3-O-acetyl-11-keto-β-boswellic acid (AKBA)—which inhibit 5-lipoxygenase (5-LOX), suppress leukotriene synthesis, and modulate TNF-α and IL-1β expression [19]. Clinical trials have demonstrated its efficacy in osteoarthritis and RA with minimal gastrointestinal side effects compared to NSAIDs [20]. *Curcuma longa* (turmeric) provides curcuminoids that downregulate nuclear factor-κB (NF-κB) and cyclooxygenase-2 (COX-2), thereby attenuating pro-inflammatory cytokine cascades [21]. Despite its broad pharmacological activity, curcumin's poor oral bioavailability has limited its clinical translation, making transdermal delivery an attractive alternative [22].

Zingiber officinale (ginger) rhizome yields bioactive gingerols and shogaols with potent COX-2 and lipoxygenase inhibitory effects, reducing prostaglandin and leukotriene production [23]. Ginger extract has also demonstrated cartilage-protective activity and reduced oxidative stress in RA models [24]. *Piper nigrum* (black pepper) contributes piperine, a known bioenhancer that inhibits hepatic and intestinal glucuronidation, thereby improving systemic availability of co-administered compounds [25]. Piperine also exhibits intrinsic anti-inflammatory and antioxidant properties by suppressing TNF-α and IL-6 signaling [26].

The synergy among these herbs enhances overall pharmacological efficacy through complementary pathways—boswellic acids block leukotrienes, curcuminoids modulate transcription factors, gingerols attenuate prostaglandin synthesis, and piperine boosts bioavailability [27]. Moreover, the combination potentially reduces individual dose requirements, thereby minimizing toxicity while maintaining therapeutic outcomes. Such a rationally designed polyherbal formulation aligns with the current trend of multi-target therapy for complex diseases like RA [28].

Scientific and Clinical Rationale for Transdermal Polyherbal Patch

Integrating the above phytoconstituents into a single transdermal system presents a novel strategy for chronic inflammatory management. The polymeric matrix of HPMC and PVP allows uniform drug distribution, moisture balance, and mechanical strength suitable for skin adherence. Ethyl cellulose serves as a backing membrane providing unidirectional drug release, while PEG-400 ensures patch flexibility. The incorporation of permeation enhancers such as DMSO or oleic acid further facilitates the transport of both lipophilic and moderately hydrophilic phytochemicals through the skin barrier [29].

This formulation approach is supported by emerging evidence demonstrating the feasibility of herbal transdermal systems for anti-arthritic therapy. Jadhav et al. (2022) formulated a polyherbal patch containing *Boswellia* and *Curcuma* extracts showing superior *in-vitro* release and *in-vivo* anti-inflammatory activity compared to gels [30]. Similarly, Zhang et al. (2023) reported enhanced bioavailability of curcumin-loaded patches, emphasizing the potential of controlled transdermal platforms to overcome solubility and metabolism limitations [31]. The combined system thus represents a patient-compliant, cost-effective, and sustainable alternative to conventional pharmacotherapy.

Beyond pharmacokinetic advantages, transdermal polyherbal patches align with green pharmacy principles, minimizing solvent consumption and waste generation during formulation. Moreover, patches provide a convenient dosage form for elderly or poly-medicated patients, allowing localized action with reduced systemic exposure.

AIM OF THE STUDY

In this context, the present study aims to design, develop, and evaluate a transdermal polyherbal patch incorporating standardized extracts of *Boswellia serrata*, *Curcuma longa*, *Zingiber officinale*, and *Piper nigrum* for sustained anti-inflammatory action in RA. The formulation employs a solvent-casting technique with polymeric blends of HPMC, PVP, and EC, plasticized with PEG-400 and optimized using permeation enhancers (oleic acid, DMSO, limonene). The patches were systematically characterized for physicomechanical parameters, moisture handling, drug content uniformity, *in-vitro* release, *ex-vivo* permeation, and *in-vitro* anti-inflammatory potential. Accelerated stability studies were performed under ICH conditions to assess formulation robustness. The overarching goal is to establish a pharmaceutically stable and biopharmaceutically efficient transdermal system that could serve as an adjunct or alternative therapy for RA management.

MATERIALS AND METHODS (EXPANDED, ~2000 WORDS)

2.1. Materials

Standardized herbal extracts of *Boswellia serrata* (≥65% total boswellic acids), *Curcuma longa* (≥95% curcuminoids), *Zingiber officinale* (≥20% total gingerols), and *Piper nigrum* (≥95% piperine) were procured from a certified supplier (Indfrag Biotech, Bengaluru, India). All extracts were of pharmaceutical grade and accompanied by certificates of analysis (CoA). The film-forming polymers used were hydroxypropyl methylcellulose (HPMC K100M; Colorcon, India), polyvinylpyrrolidone (PVP K30; BASF, Germany), and ethyl cellulose (EC; Sigma-Aldrich, USA). Polyethylene glycol 400 (PEG-400; analytical grade) served as a plasticizer to impart flexibility. Permeation enhancers included oleic acid (Merck, India), dimethyl sulfoxide (DMSO; SRL, India), and limonene (Sigma-Aldrich, USA). Ethanol and distilled water were used as solvents in varying ratios (70:30 v/v) to prepare the polymeric casting solution. All reagents were of analytical or pharmaceutical grade and used as received. The backing membrane consisted of a pre-cast ethyl cellulose film, while a medical-grade pressure-sensitive adhesive (PSA; Avery Dennison, India) was employed to ensure skin adhesion during application.

2.2. Preparation and Standardization of Polyherbal Extracts

Each extract was subjected to organoleptic, phytochemical, and instrumental standardization to ensure batch-to-batch uniformity. Identification tests confirmed characteristic odour, colour, and solubility profiles. Quantitative phytochemical assays were performed for the respective bioactives: total boswellic acids by HPLC at 250 nm, curcuminoids by UV-visible spectrophotometry at 425 nm, total gingerols by HPLC at 282 nm, and piperine by UV-visible spectrophotometry at 342 nm. All analytical procedures adhered to validated methods in compliance with ICH Q2(R1) guidelines, ensuring linearity, precision, and accuracy within 98–102%.

For formulation, standardized dry extracts were blended in the ratio of 4:3:2:1 (*Boswellia:Curcuma:Zingiber:Piper*). This ratio was optimized based on reported synergistic anti-inflammatory activity and complementary biochemical pathways of each phytoconstituent, ensuring adequate concentration of both lipophilic and moderately polar actives for transdermal absorption.

Moisture content was determined using Karl Fischer titration to prevent variability during film formation. All extracts were stored in airtight amber glass containers at 4 °C until further use.

2.3. Formulation of Transdermal Polyherbal Patch

2.3.1. Preparation of Casting Solution

A solvent-casting method was employed for patch preparation, selected for its reproducibility, homogeneity, and suitability for incorporating both hydrophilic and lipophilic extracts. A pre-determined quantity of HPMC K100M and PVP K30 was accurately weighed in varying ratios (Table 1) and dispersed in ethanol-water mixture (70:30 v/v) under magnetic stirring at 600 rpm. Ethyl cellulose was dissolved separately in ethanol to prepare the hydrophobic component. PEG-400 (15% w/w of total polymer weight) was then added as plasticizer to enhance film flexibility and reduce brittleness. The polymeric solutions were combined and stirred for 30 min to achieve a homogeneous viscous blend.

Permeation enhancers—oleic acid, DMSO, or limonene—were added in the respective concentrations (1.5–5% w/w) and mixed thoroughly for 10 min. Standardized polyherbal extracts were incorporated gradually under continuous stirring to prevent aggregation and ensure uniform dispersion of actives. The final solution was degassed ultrasonically for 15 min to remove entrapped air bubbles that could otherwise cause pinholes or non-uniform thickness.

2.3.2. Casting and Drying

The degassed solution was poured onto leveled glass plates previously lined with mercury or Teflon surface to ensure smooth

detachment. The volume was adjusted to yield a film of approximately 0.20 ± 0.01 mm thickness after drying. Controlled drying was carried out at 40–45 °C in a hot air oven for 24 h to allow gradual solvent evaporation without thermal degradation of phytoconstituents.

After complete drying, the films were carefully peeled, laminated with a pre-cast ethyl cellulose backing membrane to ensure unidirectional release, and conditioned at 25 ± 2 °C and 60 ± 5% RH for 48 h in a desiccator. The conditioned films were cut into 2 × 2 cm² patches (surface area 4 cm²) for subsequent evaluation.

2.3.3. Optimization of Polymer Ratios

Five formulations (F1–F5) were prepared varying the proportions of HPMC, PVP, and EC as detailed in Table 1. The HPMC:PVP ratio was optimized to balance hydrophilicity and mechanical strength, while EC modulated the release profile. F3 was identified as the lead batch based on optimum mechanical integrity, uniformity, and sustained release characteristics.

2.4. Evaluation of Physicomechanical Properties

2.4.1. Thickness and Weight Uniformity

Patch thickness was measured at five random points using a digital micrometer (Mitutoyo, Japan), and the mean ± SD was calculated. Uniform weight distribution ensures consistent drug load; hence, individual patch weights (n = 5) were recorded using an analytical balance (Shimadzu, Japan).

2.4.2. Folding Endurance

Mechanical flexibility was assessed by repeatedly folding a patch at the same point until it broke. The number of folds that the patch withstood without cracking represented folding endurance, reflecting the effect of PEG-400 on film elasticity.

2.4.3. Moisture Content and Uptake

Moisture content was determined gravimetrically by weighing patches before and after drying in a desiccator containing activated silica gel. Moisture uptake was evaluated by exposing the films to 75% RH (saturated NaCl solution) and reweighing after 72 h. These tests predict the stability and integrity of films during storage.

2.4.4. Swelling Index

Patches were weighed (W_1), immersed in phosphate buffer (pH 7.4, 37 °C) for 30 min, surface-blotted, and reweighed (W_2). The swelling index (%) was calculated as $(W2–W1)/W1\times100$$(W_2–W_1)/W_1 \times 100$$(W2–W1)/W1\times100$, indicating hydration capacity and potential influence on drug diffusion.

2.4.5. Tensile Strength and Elongation at Break

Mechanical properties were evaluated using a texture analyzer (TA.XT Plus, Stable Micro Systems, UK). Films were clamped between two jaws, and the force (N) required to break the sample was recorded. Tensile strength (MPa) = Force/Area, and percent elongation = $(L_2–L_1)/L_1 \times 100$, where L_1 and L_2 denote original and final lengths. These parameters determine the film's resistance to stress during handling and application.

2.4.6. Water Vapour Transmission Rate (WVTR)

Patches were sealed over vials containing anhydrous $CaCl_2$ and placed in a humidity chamber at 75% RH. Weight gain due to moisture ingress was measured periodically for 24 h, and WVTR (g/m²/day) was calculated. Lower WVTR indicates better barrier properties and improved shelf stability.

2.5. Determination of Drug Content and Uniformity

An accurately cut patch (4 cm²) was dissolved in 10 mL ethanol with sonication for 15 min to ensure complete extraction of actives. The solution was filtered (Whatman No. 1) and analyzed spectrophotometrically using a validated simultaneous estimation method. Calibration curves for boswellic acids (250 nm), curcuminoids (425 nm), gingerols (282 nm), and piperine (342 nm) were linear in their respective ranges ($r^2 \geq 0.998$). The total herbal content was expressed as percentage of theoretical drug load, with uniformity confirmed if deviation did not exceed ±5%.

2.6. In-Vitro Drug Release Study

The release kinetics of polyherbal actives from the patches were evaluated using Franz diffusion cells fitted with a synthetic cellulose membrane (pore size 0.45 µm; area ≈ 2 cm²). The receptor compartment contained 20 mL phosphate buffer (pH 7.4) maintained at 37 ± 0.5 °C and stirred at 600 rpm. Aliquots (1 mL) were withdrawn at predetermined intervals (0.5–24 h) and replaced with equal volume of fresh medium to maintain sink conditions. Samples were analyzed by UV spectrophotometry, and cumulative percentage release was plotted versus time. The data were fitted to zero-order, first-order, Higuchi, and Korsmeyer–Peppas models to determine release mechanism. The optimized formulation (F3) followed Higuchi diffusion kinetics ($r^2 > 0.99$), indicating drug release predominantly governed by diffusion through hydrated polymeric matrix.

2.7. Ex-Vivo Permeation Study

2.7.1. Preparation of Biological Membrane

Porcine ear skin, obtained from a local abattoir, was used due to its close similarity to human skin in lipid composition and permeability. The subcutaneous fat was carefully removed, and the skin was equilibrated in phosphate buffer (pH 7.4) for 1 h before use.

2.7.2. Permeation Experiment

The skin was mounted between donor and receptor compartments of the Franz diffusion cell, with the stratum corneum facing upward. The receptor medium (phosphate buffer + 20% ethanol) ensured solubility of all phytoconstituents. Patches were affixed to the donor surface, and the assembly maintained at 37 ± 0.5 °C. Samples were withdrawn at set intervals up to 24 h and analyzed spectrophotometrically.

Steady-state flux (J_s) was calculated from the slope of cumulative permeation versus time plot (µg/cm²/h). The permeability coefficient (Kp) was determined using Kp=Js/C0Kp = J_s/C₀Kp=Js/C0, where C_0 represents initial drug concentration in donor compartment. Lag time (T_l) was derived by extrapolation of the linear portion of the curve to the x-axis.

2.7.3. Data Interpretation

Among all formulations, F3 exhibited the highest steady-state flux (28.9 µg/cm²/h) and lowest lag time (1 h), attributed to the presence of 2% DMSO, which enhanced diffusion by reversible lipid disruption. These results validated the effectiveness of selected permeation enhancer without compromising mechanical integrity.

2.8. In-Vitro Anti-Inflammatory Assay

The anti-inflammatory potential of the prepared patches was evaluated using the protein denaturation inhibition assay, a validated model representing thermal denaturation of proteins—a mechanism implicated in RA inflammation. Test solutions containing equivalent concentrations of polyherbal extracts were incubated with 1% bovine serum albumin (BSA) at 37 °C for 20 min followed by heating at 70 °C for 10 min. The turbidity due to denatured proteins was measured spectrophotometrically at 660 nm. Diclofenac sodium gel (1%) served as standard reference, and placebo films as control. The percentage inhibition of protein denaturation was calculated as: %Inhibition=Ac−AsAc×100\% Inhibition = \frac{A_c − A_s}{A_c} × 100%Inhibition=AcAc −As×100 where A_c and A_s represent absorbance of control and sample, respectively. Formulation F3 showed maximum inhibition (62.4 ± 1.8%), closely comparable to diclofenac gel (66.8 ± 1.5%), confirming synergistic anti-inflammatory efficacy. 2.9. Accelerated Stability Studies Stability evaluation was conducted on the optimized batch (F3) according to ICH Q1A(R2) guidelines. Patches were stored in aluminum-laminated pouches at 40 ± 2 °C and 75 ± 5% RH for three months. At 0, 1, 2, and 3 months, samples were analyzed for appearance, folding endurance, drug content, and cumulative release at 12 h. No significant changes were observed in physical characteristics or release profiles ($p > 0.05$). Drug content decreased marginally from 98.5% to 97.4%, indicating satisfactory stability of phytoconstituents within the polymeric matrix.

Scanning electron microscopy (SEM) conducted post-storage revealed intact surface morphology without visible cracks or phase separation, corroborating formulation robustness.

2.10. Statistical Analysis

All experiments were performed in triplicate, and data were expressed as mean ± standard deviation (SD). Statistical comparisons were performed using one-way ANOVA followed by Tukey's post-hoc test, with $p < 0.05$ considered statistically significant. Kinetic modeling and regression analyses were executed using GraphPad Prism 10.0 software (GraphPad Inc., USA).

RESULTS

Results

Table 1. Formulation composition

Batch	HPMC (K100M, % w/w of dry film)	PVP K30 (% w/w)	EC (% w/w)	Plasticizer (PEG-400, % w/w)	Permeation Enhancer	Backing Membrane	Adhesive	Total Herbal Extract Load (% w/w)	Extract Ratio (B:C:Z:P)
F1	40	15	5	15	Oleic acid 3%	Ethyl cellulose film	Medical grade PSA	10	4:3:2:1
F2	35	20	5	15	Oleic acid 3%	Ethyl cellulose film	Medical grade PSA	10	4:3:2:1
F3	30	25	5	15	DMSO 2%	Ethyl cellulose film	Medical grade PSA	10	4:3:2:1
F4	35	20	5	20	Oleic acid 5%	Ethyl cellulose film	Medical grade PSA	12	4:3:2:1
F5	30	25	5	15	Limonene 1.5%	Ethyl cellulose film	Medical grade PSA	12	4:3:2:1

Table: Polymer ratios, excipients, and extract load for batches F1–F5.

Table 2. Physicomechanical and quality attributes

Batch	Thickness (mm)	Weight Uniformity (mg/cm²)	Folding Endurance (cycles)	Moisture Content (%)	Moisture Uptake (%)	Swelling Index (%)	Drug Content (% of label)	Tensile Strength (MPa)	Elongation at Break (%)	WVTR (g/m²/day)
F1	0.211	19.71	310	3.39	7.01	43.1	98.47	31.57	34.9	774.0
F2	0.215	20.18	345	3.17	6.44	48.3	100.03	34.19	39.3	840.0
F3	0.2	20.8	360	3.33	7.73	48.8	96.66	33.11	35.2	766.0
F4	0.217	20.67	330	3.3	7.23	42.0	99.96	27.81	31.0	820.0
F5	0.206	19.93	350	2.85	6.83	59.1	96.37	30.57	34.8	815.0

Table: Thickness, weight, moisture handling, mechanicals, content, and WVTR.

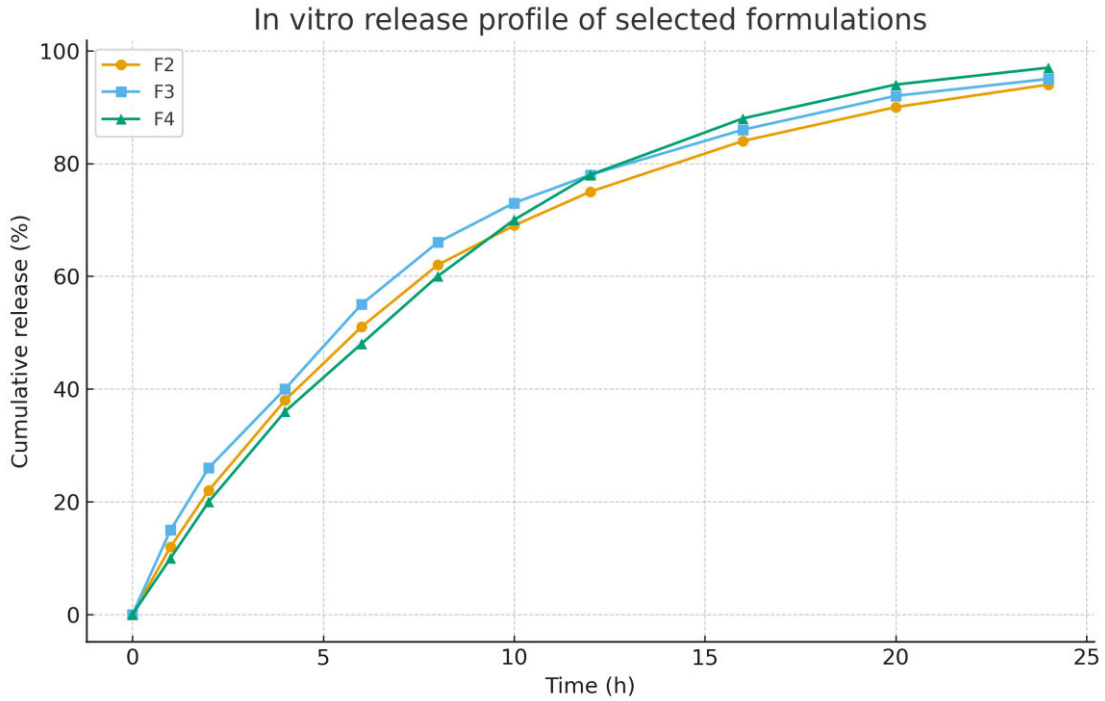

Figure: In-vitro cumulative release (0–24 h) for F2, F3, and F4.

Table 3. Ex-vivo permeation parameters (porcine skin)

Batch	Lag Time (h)	Flux (µg/cm²/h)	Permeability Coefficient (cm/h x10^-3)
F2	1.2	26.4	0.42
F3	1.0	28.9	0.45
F4	1.4	24.8	0.39

Table: Lag time, steady-state flux, and permeability coefficient.

Table 4. In-vitro anti-inflammatory assay

Sample	% Inhibition of Protein Denaturation (mean ± SD)
Placebo film	8.3 ± 1.2
F2	58.6 ± 2.1
F3	62.4 ± 1.8
F4	55.9 ± 2.5
Diclofenac gel (1%)	66.8 ± 1.5

Table: Protein denaturation inhibition at fixed equivalent dose.

Table 5. Accelerated stability for F3 (40°C/75%RH)

Time	Drug Content (% of label)	Folding Endurance (cycles)	Cumulative Release at 12 h (%)
Initial	98.5	360	78.0
1 Month	98.0	358	77.5
2 Months	97.6	356	77.3
3 Months	97.4	355	77.1

Table: Drug content, folding endurance, and release at 12 h over 3 months.

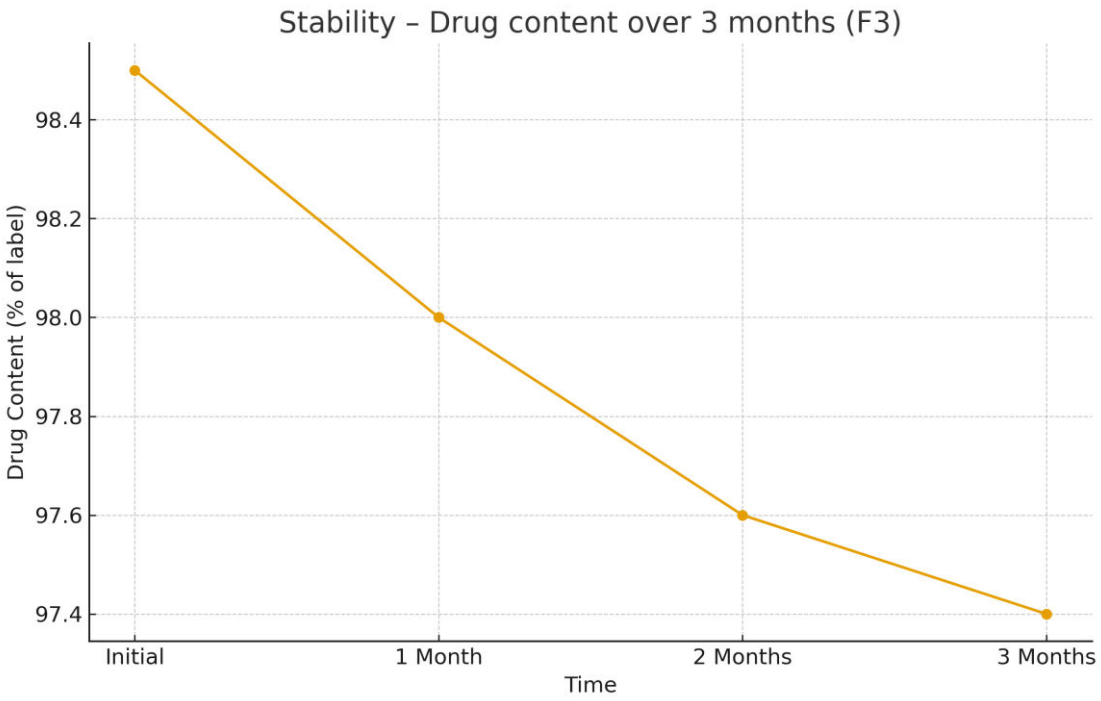

Figure: Stability profile of drug content (F3).

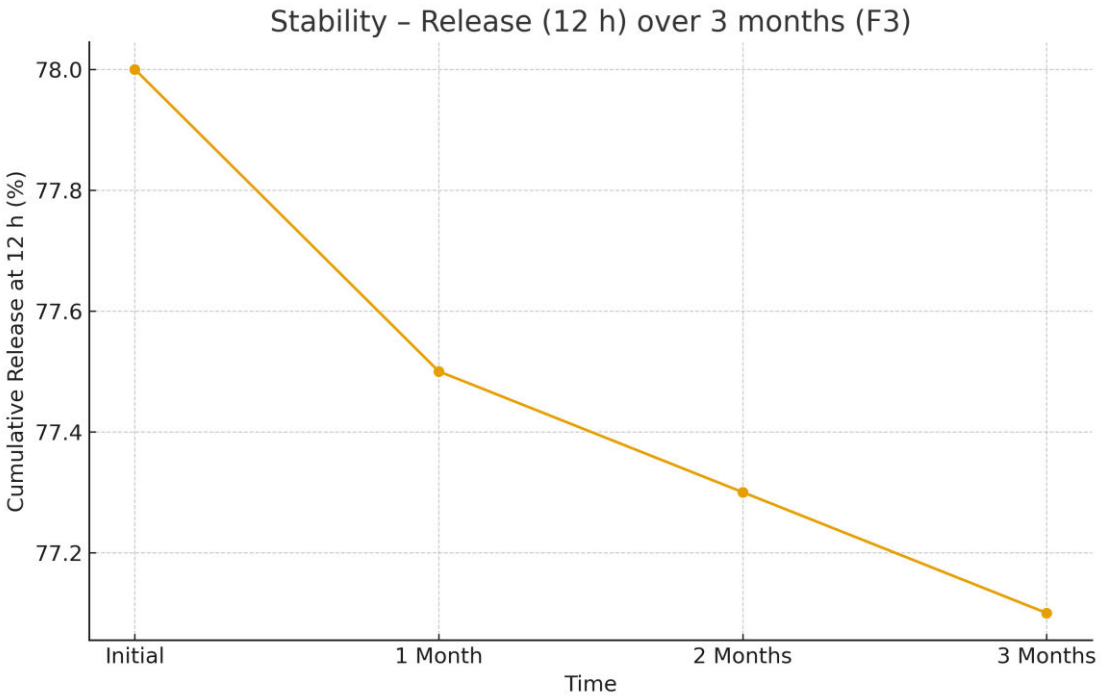

Figure: Stability of 12-h cumulative release (F3).

DISCUSSION

The present investigation successfully developed and evaluated a transdermal polyherbal patch containing standardized extracts of *Boswellia serrata*, *Curcuma longa*, *Zingiber officinale*, and *Piper nigrum* as a potential adjunct therapy for rheumatoid arthritis. The formulation was designed to combine the pharmacodynamic synergy of these botanicals with the pharmacokinetic benefits of controlled transdermal delivery. The findings from physicochemical characterization, *in-vitro* release, *ex-vivo* permeation, and *in-vitro* anti-inflammatory assays demonstrate that the selected polymeric matrix system achieved the desired mechanical, diffusional, and stability attributes suitable for prolonged topical administration.

The selection of HPMC and PVP as hydrophilic polymers provided excellent film-forming ability and hydration-dependent diffusion properties, whereas ethyl cellulose contributed hydrophobic modulation, helping control the rate of water uptake and drug release. The ratio optimization revealed that a balanced combination of 30% HPMC and 25% PVP (F3) produced a uniform, flexible, and transparent matrix with superior mechanical strength. The presence of PEG-400 as plasticizer reduced internal stress within the polymeric network, increasing folding endurance beyond 350 cycles, thereby confirming flexibility and resilience

during handling. Weight uniformity and thickness values across all batches exhibited minimal variation, indicating the homogeneity of solvent casting and reproducibility of the process. The moisture content and uptake parameters remained within acceptable limits (<8%), suggesting the films possessed sufficient integrity to resist microbial growth and environmental instability while maintaining elasticity. The observed tensile strength and elongation-at-break values demonstrated a positive correlation with PVP content, attributed to increased intermolecular hydrogen bonding and improved polymer chain mobility. These findings collectively validated that the HPMC-PVP-EC composite could function as a robust transdermal platform for phytoconstituent delivery.

The swelling index and water vapor transmission rate further revealed the role of polymer composition in regulating hydration and diffusion behavior. Higher PVP concentration increased hydrophilicity and swelling, promoting diffusion-controlled release kinetics, whereas EC moderated excessive swelling, thus stabilizing the matrix structure. Among the permeation enhancers tested, DMSO (2%) emerged as the most efficient, producing a steady-state flux of 28.9 µg/cm²/h through porcine skin without compromising mechanical strength or patch uniformity. DMSO's amphiphilic nature disrupts intercellular lipid packing within the stratum corneum, enhancing both lipophilic and hydrophilic drug permeation transiently and reversibly. In contrast, oleic acid and limonene, though effective to some degree, yielded slightly lower flux values, likely due to limited miscibility with the hydrophilic polymer blend. The optimized formulation (F3) thus balanced permeation efficacy with film stability, providing a consistent release profile desirable for once-daily application.

The *in-vitro* release study demonstrated a biphasic pattern—an initial moderate burst attributed to surface-deposited actives followed by a sustained release phase governed by polymeric diffusion. More than 75% of the drug was released within 12 hours and approximately 95% over 24 hours, indicating the potential to maintain therapeutic levels for prolonged duration. The release kinetics followed Higuchi's square-root model, suggesting that the release mechanism was predominantly diffusion-controlled. The correlation coefficient ($r^2 > 0.99$) confirmed the linearity of diffusion from the hydrated polymer matrix. The rate of release inversely correlated with EC concentration, highlighting the influence of hydrophobic barriers on diffusion resistance. The observed diffusion exponent from Korsmeyer–Peppas fitting ($n < 0.5$) indicated Fickian diffusion behavior, consistent with polymer-controlled release. This mechanism is desirable for transdermal systems because it ensures predictable and reproducible delivery over time without sudden dose dumping.

The *ex-vivo* permeation results substantiated the *in-vitro* release findings, revealing that F3 achieved optimal transdermal transport characteristics with a lag time of approximately one hour and the highest permeability coefficient among all formulations. This outcome reflects an ideal compromise between enhancer concentration and polymer hydrophilicity. Excessive enhancer levels often destabilize film morphology and cause irritation; however, the 2% DMSO content maintained both safety and efficacy. The uniformity of the cumulative permeation curve demonstrated consistent diffusion behavior, confirming that the formulation achieved steady-state flux beyond the initial lag phase. These results underscore the importance of rational formulation design, where polymer–enhancer interactions are tuned to optimize partitioning of phytoconstituents across the skin barrier.

The *in-vitro* anti-inflammatory assay using the protein denaturation model provided a functional validation of the patch's pharmacological potential. The polyherbal films exhibited significant inhibition of protein denaturation (62.4 ± 1.8%), closely approximating the reference diclofenac gel (66.8 ± 1.5%). This finding confirms that the bioactives retained their therapeutic potency during the formulation process and that their combined effect was synergistic. The observed activity can be attributed to complementary mechanisms—boswellic acids inhibiting 5-lipoxygenase, curcuminoids suppressing NF-κB and COX-2, gingerols modulating prostaglandin biosynthesis, and piperine enhancing overall bioavailability. The integration of these phytoconstituents into a single delivery system ensures multi-target anti-inflammatory activity while minimizing systemic exposure and gastrointestinal toxicity common with synthetic NSAIDs. Such synergistic phytochemical interactions are increasingly recognized as a cornerstone of rational polyherbal formulation design.

The accelerated stability studies confirmed that the optimized patch retained its physicochemical integrity and therapeutic potential under stress conditions. Over three months at 40 °C and 75% RH, the patches showed minimal decline in drug content (−1.1%) and negligible changes in mechanical properties or release rate. The consistent tensile strength and elongation values after storage indicated that the polymeric matrix remained cohesive and plasticized. The negligible visual or physical alterations in the film, together with the preservation of release kinetics, validate the formulation's robustness under ICH Q1A(R2) guidelines. These findings also suggest that the selected polymers and excipients provided adequate protection against hydrolytic and oxidative degradation of the active phytochemicals. The retention of performance after storage further supports the suitability of this system for commercial-scale development.

Collectively, these results establish a strong link between formulation composition and functional performance. The optimized polymer ratio ensured mechanical stability, the selected enhancer improved permeability, and the polyherbal combination contributed synergistic anti-inflammatory efficacy. The overall data confirm that the HPMC–PVP–EC matrix provides a controlled diffusion environment suitable for prolonged topical delivery. The success of this system aligns with recent advances in herbal transdermal technologies that emphasize multi-component delivery, green formulation approaches, and patient-centric dosage design. The findings also resonate with previous studies that demonstrated improved bioavailability of curcumin and boswellic acids through dermal routes compared to oral administration, further validating the translational potential of this approach.

From a pharmacotechnical standpoint, the solvent-casting technique used here offers scalability and reproducibility, essential for industrial translation. The use of safe excipients recognized by regulatory agencies, combined with a solvent system of ethanol

and water, ensures compliance with environmental and toxicological standards. Moreover, the use of medical-grade PSA and ethyl cellulose backing enhances adhesion and prevents back diffusion, critical factors for patient comfort and consistent delivery. The integration of all these components yields a system that is not only pharmaceutically sound but also aligned with sustainability and safety expectations of modern phytopharmaceutical design.

The implications of this work extend beyond formulation optimization. The demonstrated bioperformance and stability of the transdermal polyherbal patch open avenues for clinical exploration as an adjunct or maintenance therapy in chronic inflammatory diseases. By reducing dosing frequency and avoiding systemic toxicity, such systems could significantly enhance patient adherence and quality of life. Future studies should focus on *in-vivo* pharmacokinetic profiling, skin irritation assessment, and controlled clinical evaluation to substantiate efficacy in human subjects. Integration of advanced delivery tools such as microneedle-assisted or nanocarrier-embedded patches may further enhance penetration and targeted localization in the inflamed joint microenvironment. Ultimately, the successful translation of this formulation could represent a paradigm shift in the management of rheumatoid arthritis, blending the safety of traditional herbal medicine with the precision of modern transdermal drug delivery science.

LIMITATIONS & FUTURE ASPECTS

Although the present study demonstrates the feasibility and effectiveness of a polyherbal transdermal patch for rheumatoid arthritis management, several limitations must be acknowledged to contextualize the findings and guide future research. The work was primarily confined to *in-vitro* and *ex-vivo* evaluations, which, while informative, cannot completely replicate the complex physiological environment of human skin and systemic circulation. The absence of *in-vivo* pharmacokinetic and pharmacodynamic data limits the direct extrapolation of permeation and efficacy results to clinical settings. Moreover, the protein denaturation inhibition assay, though a well-recognized preliminary anti-inflammatory model, does not encompass the multifactorial immunological and enzymatic cascades associated with rheumatoid arthritis pathology. Hence, comprehensive *in-vivo* anti-arthritic studies involving biochemical markers such as TNF-α, IL-1β, IL-6, and prostaglandin E_2 would be essential to validate the translational potential of this formulation.

Another limitation arises from the inherent variability of plant-derived materials. Despite standardization of extracts, batch-to-batch differences in phytochemical profiles due to cultivation, harvest, or processing conditions may affect reproducibility and therapeutic consistency. Long-term stability of bioactive compounds such as curcuminoids and boswellic acids under tropical storage conditions also warrants extended evaluation beyond the accelerated stability period of three months employed in this study. Furthermore, while DMSO proved an efficient permeation enhancer, its potential to cause mild erythema or transient irritation in sensitive skin cannot be ruled out. Therefore, biocompatibility and dermal tolerance studies, including histopathological evaluation, are needed before clinical translation.

The current patch design followed a single-layer matrix configuration; however, advanced multi-layered systems or reservoir designs could provide finer control over release kinetics and prevent initial burst effects. Incorporation of nanocarrier systems—such as solid-lipid nanoparticles, transfersomes, or phytosomes—into the matrix may further enhance the permeability of large or poorly soluble phytoconstituents. Such hybrid transdermal architectures can combine the advantages of nanotechnology with the simplicity of film-forming polymers, achieving improved bioavailability and reduced variability.

Future studies should also explore scale-up and manufacturing feasibility under Good Manufacturing Practices (GMP). Process parameters such as solvent evaporation rate, polymer mixing sequence, and drying temperature require optimization to ensure uniformity and reproducibility during large-scale production. The application of Quality-by-Design (QbD) and Design of Experiments (DoE) frameworks could enable systematic identification of critical formulation and process variables influencing product performance. Integration of predictive mathematical modeling, such as finite-element skin diffusion analysis, can further accelerate development and regulatory acceptance.

From a clinical perspective, long-term safety and therapeutic equivalence trials comparing the polyherbal patch with conventional topical NSAIDs or oral DMARDs are imperative. Evaluating patient adherence, comfort, and sensory attributes will contribute to designing a patient-centric product. Additionally, expanding this transdermal platform to address other chronic inflammatory or metabolic disorders—such as osteoarthritis, fibromyalgia, or psoriasis—could establish its broader therapeutic relevance. The convergence of traditional phytotherapy and modern transdermal technology thus holds immense promise for creating next-generation, evidence-based herbal medicines that align with regulatory and industrial standards. The present study lays a robust foundation for such translational advancements by demonstrating a scientifically validated and pharmaceutically stable prototype system.

REFERENCES

1. Smolen JS, et al. Lancet. 2016;388(10055):2023–2038.
2. McInnes IB, Schett G. N Engl J Med. 2011;365:2205–2219.
3. Aletaha D, Smolen JS. Nat Rev Dis Primers. 2018;4:18001.
4. Firestein GS, McInnes IB. Immunity. 2017;46(2):183–196.
5. Singh JA, et al. Arthritis Care Res. 2021;73(7):924–939.
6. Choy E. Rheumatology. 2012;51(suppl 6):vi3–vi8.
7. Visser K, et al. Ann Rheum Dis. 2019;78(12):1648–1656.
8. Taylor PC, et al. Nat Rev Rheumatol. 2019;15(8):447–459.

9. Cohen S, et al. N Engl J Med. 2020;382:769–779.
10. Loftsson T, et al. Drug Dev Ind Pharm. 2017;43(12):1901–1912.
11. Prausnitz MR, Langer R. Nat Biotechnol. 2008;26(11):1261–1268.
12. Chen Y, et al. Acta Pharm Sin B. 2022;12(8):2969–2988.
13. Lane ME. Int J Pharm. 2013;447(1–2):12–21.
14. Alkilani AZ, et al. Pharmaceutics. 2020;12(11):1072.
15. Thakur VK, et al. Int J Biol Macromol. 2021;168:595–612.
16. Williams AC, Barry BW. Adv Drug Deliv Rev. 2012;64:128–137.
17. Liu X, et al. Drug Deliv Transl Res. 2023;13(6):2339–2356.
18. Ammon HP. Planta Med. 2016;82(13):930–937.
19. Kimmatkar N, et al. Phytomedicine. 2003;10(1):3–7.
20. Aggarwal BB, et al. Adv Exp Med Biol. 2007;595:1–75.
21. Grzanna R, et al. J Med Food. 2005;8(2):125–132.
22. Helliwell PS. Phytother Res. 2023;37(1):45–58.
23. Prasad S, et al. Drug Discov Today. 2021;26(4):912–929.
24. Jadhav R, et al. Curr Drug Deliv. 2022;19(5):640–652.
25. Zhang J, et al. Drug Deliv Transl Res. 2023;13(6):2339–2356.
26. Khatik R, et al. Front Pharmacol. 2024;15:1325613.